Research Article | Vol. 9, No. 12 | 1 Dec 2018 | BIOMEDICAL OPTICS EXPRESS 5982
Biomedical Optics EXPRESS

Within-subject assessment of foveal avascular zone enlargement in different stages of diabetic retinopathy using *en face* OCT reflectance and OCT angiography

GISELLE LYNCH,[1,2] JORGE S. ANDRADE ROMO,[1] RACHEL LINDERMAN,[3] BRIAN D. KRAWITZ,[1] SHELLEY MO,[1] AMIR ZAKIK,[1] JOSEPH CARROLL,[3,4] RICHARD B. ROSEN,[1,2] AND TOCO Y. P. CHUI[1,2,*]

[1]*Ophthalmology, New York Eye and Ear Infirmary of Mount Sinai, 310 East 14th St., Suite 500, S. Bldg., New York, NY, 10003, USA*
[2]*Icahn School of Medicine at Mount Sinai, 1 Gustave L. Levy Pl, New York, NY, 10029, USA*
[3]*Cell Biology, Neurobiology & Anatomy, Medical College of Wisconsin, 8701 Watertown Plank Rd., Milwaukee, WI, 53226, USA*
[4]*Ophthalmology & Visual Sciences, Medical College of Wisconsin, 925 N. 87th St., Milwaukee, WI, 53226, USA*
**ychui@nyee.edu*

Abstract: Enlargement of the foveal avascular zone (FAZ) due to progressive capillary nonperfusion is associated with visual deterioration in patients with diabetic retinopathy. The FAZ area has long been considered an important clinical marker of advancing retinopathy. However, a large body of literature shows that the FAZ area varies considerably in healthy eyes, resulting in substantial overlap between controls and diabetics, thus reducing its discriminatory value. In this study, within-subject FAZ area enlargement was obtained by the comparison of the structural FAZ area to the functional FAZ area using simultaneously-acquired, corresponding *en face* OCT reflectance and OCT angiography images. Our study suggests that *en face* OCT reflectance images provide useful anatomic baselines of structural FAZ morphology prior to the onset of disease. Measurements of within-subject FAZ area enlargement appear to be a more sensitive method for identifying the onset of diabetic retinopathy as compared to using OCT angiographic measurements of FAZ alone.

1. Introduction

Diabetic retinopathy is the most common microvascular complication of diabetes, and remains a leading cause of blindness worldwide [1–4]. A number of studies using intravenous fluorescein angiography (IVFA) or optical coherence tomography (OCT) angiography have utilized the detection of retinal vascular abnormalities and foveal avascular zone (FAZ) enlargement to assess the severity of diabetic retinopathy [5–13]. Altered configuration and enlargement of the FAZ has shown strong correlation with poorer visual outcomes and diabetic retinopathy progression [14–16], making quantification of FAZ dimensions increasingly important for assessment of clinical severity and predicting prognosis in diabetic retinopathy.

While IVFA detection of retinal capillary perfusion and nonperfusion has been the standard for grading diabetic retinopathy [11,12,17,18], it provides limited resolution of retinal capillary networks with minimal quantitative information [19–21]. Frequent repeated follow-up IVFA examinations are also challenging to obtain [22,23]. OCT angiography is a recently developed noninvasive alternative to IVFA which utilizes erythrocyte motion as intrinsic contrast to produce high-resolution images of the retinal microvasculature [10,24–28]. Using averaged OCT angiography images, perfused retinal capillaries appear as discrete

#345996 https://doi.org/10.1364/BOE.9.005982
Journal © 2018 Received 17 Sep 2018; revised 27 Oct 2018; accepted 28 Oct 2018; published 5 Nov 2018

Biomedical Optics EXPRESS

and continuous, allowing precise delineation of FAZ border without the noise of background fluorescence or the temporal decay of the fluorescence signal in patients with diabetic retinopathy [29–31]. *En face* OCT reflectance images can also reveal capillaries not seen on OCT angiography by utilizing the reflective microstructural information which includes both the perfused and nonperfused capillaries [32,33]. However, vascular studies using *en face* OCT reflectance have been all but non-existent due to the relative lack of contrast and the difficulty extracting clean capillary images from the full structural volume. Image registration and averaging are methods of feature enhancement which appear promising for extracting the structural detail of the vasculature needed to reveal nonperfused vessels [29,34].

The purpose of this study was to compare averaged simultaneously-acquired, corresponding *en face* OCT reflectance images to identify the baseline structural FAZ, with OCT angiographic images of the functional FAZ. We evaluated differences in FAZ area, perimeter, and acircularity index between the structural and functional FAZ, and measured within-subject FAZ area enlargement in patients with different stages of diabetic retinopathy.

2. Materials and methods

2.1 Subjects

This study was conducted at the New York Eye and Ear Infirmary of Mount Sinai and the Medical College of Wisconsin. The research study adhered to the tenets of the Declaration of Helsinki and was approved by the Institutional Review Board of the New York Eye and Ear Infirmary of Mount Sinai and the Medical College of Wisconsin (PRO 23999). Written informed consent was obtained from all subjects following discussion of the study methodology along with associated risks and benefits. A total of 117 subjects were recruited in this study. Fifteen of the controls were recruited at the Medical College of Wisconsin, all other study participants being recruited at the New York Eye and Ear Infirmary of Mount Sinai. Diabetic patient diagnoses were determined through a comprehensive chart review. Diabetic eyes were divided into three groups according to state of disease on the day of imaging, utilizing the Early Treatment Diabetic Retinopathy Study (ETDRS) classification [11,35,36]. The groups were patients with diabetes but no clinically observable diabetic retinopathy (noDR), nonproliferative diabetic retinopathy (NPDR), and proliferative diabetic retinopathy (PDR). Inclusion criteria for diabetic patients were clear natural lens, best corrected visual acuity (BCVA) better than 20/80, good fixation, and pupil dilation to at least 5mm. Exclusion criteria included presence of nystagmus, active anterior chamber inflammation, moderate to severe macular edema, pseudophakia, or prior ocular surgery. Patients were also excluded if they had additional systemic vascular diseases including HIV, uncontrolled hypertension or sickle cell disease. Inclusion and exclusion criteria for healthy controls were identical, but subjects were required to have no diabetes or any prior retinal pathology.

At the time of OCT angiography imaging, all diabetic patients had undergone a complete ophthalmic examination by an ophthalmologist, including BCVA testing, slit lamp biomicroscopy, and dilated fundoscopy. For subjects in whom both eyes met inclusion criteria, a single eye was randomly selected for inclusion in the study. A mean of 5 axial length measurements was obtained from each subject using an IOL Master (Carl Zeiss Meditec, Inc., Dublin, CA, USA). Individual retinal magnification correction for all measurements was then performed using the Littmann formula [37].

2.2 En face OCT reflectance and OCT angiography image acquisition

Images were obtained with a commercial spectral-domain OCT system (Avanti RTVue-XR; Optovue, Fremont, CA, USA), with a scan rate of 70,000 A-scans per second, scan beam centered at 840 nm, and a bandwidth of 45 nm. During the imaging session, each patient underwent 10 sequential 3x3 mm scans centered at the fovea [29,38]. A short break was given

Biomedical Optics EXPRESS

to the subject after 2-3 OCT scans or as needed. The total image acquisition time was approximately 10 minutes. Following image acquisition, *en face* OCT reflectance and corresponding OCT angiography images were generated using the native Optovue AngioVue software (Angioanalytics, versions 2016.2.0.16 and 2016.2.0.3). *En face* OCT reflectance images were generated using the mean projection of the reflectance signal, while the OCT angiograms were generated using the split-spectrum amplitude decorrelation angiography algorithm [39]. For the purpose of this study, only the superficial OCT reflectance and OCT angiography layer located between the inner limiting membrane and 15μm below the inner plexiform layer were included for further image processing and analysis. This superficial layer was studied due to the likelihood of capture the entire single-layered capillary network forming the FAZ border is high. In addition, better capillary contrast on the superficial OCT reflectance image could be achieved by excluding the background signal from the deep layer non-vascular structure. Subjects with the presence of exudates or significant macular edema that distorted the FAZ border on either the OCT reflectance or the corresponding OCT angiography images were excluded for the purpose of precise FAZ segmentation.

2.3 Image registration and averaging

In order to enhance the visualization of the FAZ border and increase the signal-to-noise ratio of each image, image registration and averaging were performed on the OCT reflectance and the OCT angiography images [29,38]. Data published previously have demonstrated that this image processing approach allows for removal of some image artifacts, such as eye motion artifacts and discontinuous vessel segments [38]. In this study, a set of 10 superficial OCT reflectance and corresponding superficial OCT angiography images without significant motion artifact (e.g. vessel doubling, blinking artifact, or major eye movement) were obtained for each subject. For each set of 10 OCT angiography images, a reference image with minimal motion artifact and highest image contrast was selected manually by a single observer. The remaining 9 OCT angiography images were then registered to this reference image using the Register Virtual Stack Slices plug-in on ImageJ (ImageJ, U. S. National Institutes of Health, Bethesda, Maryland, USA) [40]; we applied a rigid extraction model with elastic bUnwarpJ splines registration [41]. The same transformation matrix from this set of superficial OCT angiography images was then applied to the corresponding superficial OCT reflectance images using the Transform Virtual Stack Slices plug-in on ImageJ. Both registered OCT reflectance and OCT angiography images were then averaged for FAZ border delineation (Fig. 1).

Biomedical Optics EXPRESS

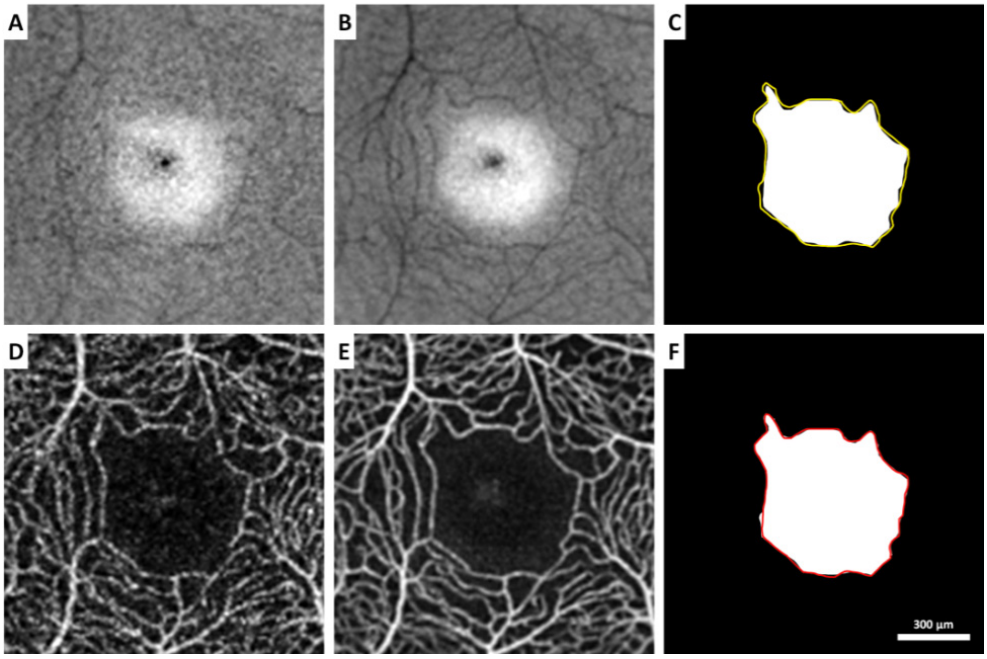

Fig. 1. (A & D) Single frame and (B & E) averaged contrast-inverted *en face* OCT reflectance and averaged OCT angiography images in a control subject. Structural and functional FAZs were manually delineated on B & E, respectively. (C & F) Structural and functional FAZ masks (white area) overlaid with functional (in yellow) and structural (in red) FAZ borders, respectively.

2.4 Structural and functional FAZ delineation

FAZ borders on the averaged contrast-inverted OCT reflectance and the averaged OCT angiography image were manually delineated using Adobe Photoshop (Adobe Systems, Inc., San Jose, CA, USA). The FAZ border on the averaged inverted-contrast OCT reflectance image was defined as capillary structure bordering the FAZ with hyporeflective cord-like appearance and complete continuity within and between capillaries. An FAZ mask was then created based on the FAZ border delineation. Structural FAZ was defined as the FAZ border delineated on the averaged OCT reflectance image and functional FAZ was defined as the FAZ border delineated on the averaged OCT angiography image. FAZ area, perimeter, and acircularity index of the structural and functional FAZs were then measured on the FAZ masks using MATLAB (The MathWorks Inc., Natick, MA) [42]. Acircularity index was computed as the ratio of the perimeter of the FAZ to the perimeter of a perfect circle with equal area [42]. A second independent grader delineated the FAZ borders on all subjects for intergrader agreement analysis.

2.5 Within-subject FAZ area enlargements

For each subject, FAZ area enlargement was computed as the difference between the structural and functional FAZ area. Quadrant and hemifield analyses of the FAZ area enlargement was performed based on the centroid of the structural FAZ, which was defined as the center of mass measured on the averaged superficial OCT reflectance image (Fig. 2). In quadrant analysis, FAZ area enlargement was divided into temporal quadrant, nasal quadrant, superior quadrant, and inferior quadrant. In hemifield analysis, FAZ area enlargement was divided into temporal hemifield, nasal hemifield, superior hemifield, and inferior hemifield.

Biomedical Optics EXPRESS

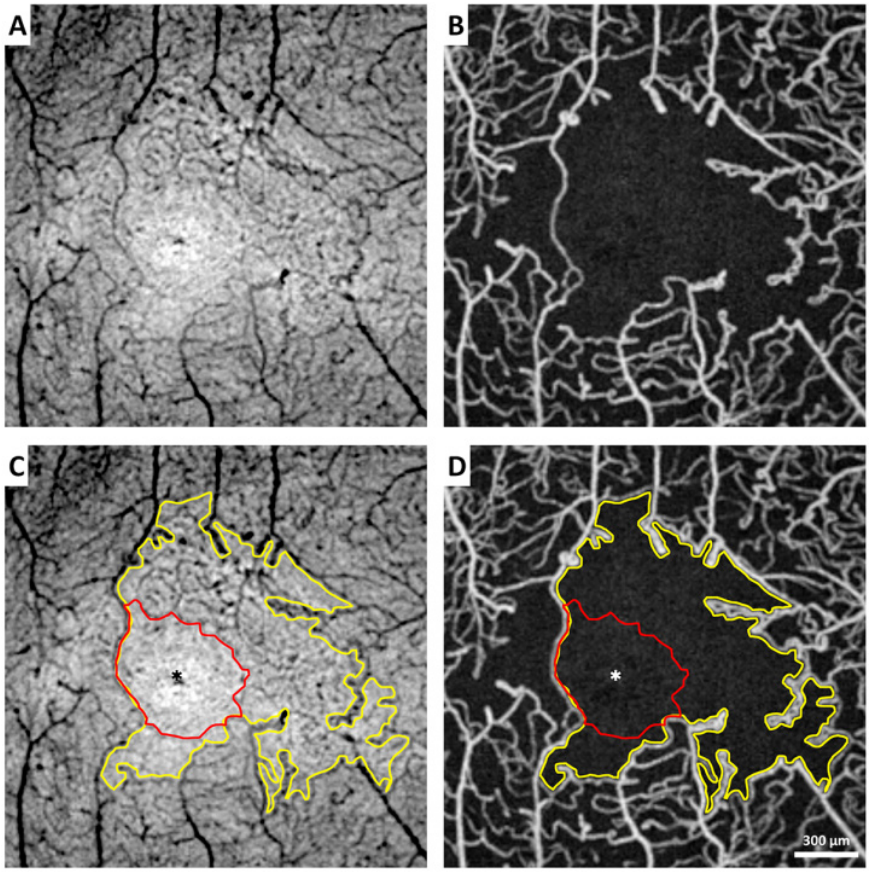

Fig. 2. Comparison of (A) contrast-inverted *en face* OCT reflectance and (B) corresponding OCT angiography image in the right eye of a PDR patient. FAZ area enlargement was measured by comparing the structural FAZ delineated on the contrast-inverted *en face* OCT reflectance and functional FAZ delineated on the OCT angiography image. (C & D) Superimposed structural FAZ (in red) and functional FAZ (in yellow) on A & B. Asterisks indicate the centroid of the structural FAZ.

2.6 Identification of nonperfused capillaries

Prior studies have shown that blood vessel structure can be visualized on the *en face* OCT reflectance images [28,32]. In this study, a non-perfused capillary segment was identified as a hypo-reflective cord-like structure on the contrast-inverted *en face* OCT reflectance image that was absent on the corresponding OCT angiography image [33].

2.7 Statistical analysis

All statistical analyses were performed using SPSS 24.0 (IBM Corporation, Chicago, IL). The intraclass correlation coefficient (ICC) with 95% confidence interval was calculated to assess intergrader agreement on FAZ area, perimeter, and acircularity index measured on both the structural and functional FAZs. Biases of FAZ area, perimeter, and acircularity index measurements between two graders were analyzed using Bland-Altman plots. FAZ area, perimeter, acircularity index, and within-subject FAZ area enlargement were all tested for normality in each study group using a Kolmogorov-Smirnov test. Since not all groups met the requirement for normality, comparison between groups using the nonparametric Kruskal-Wallis and post-hoc tests with the Bonferroni correction for multiple comparisons. Difference between the structural and functional FAZ area in the control group was compared using

Biomedical Optics EXPRESS

Wilcoxon signed-rank test. Differences between the FAZ area enlargement of the opposite quadrants and hemifields were compared using Wilcoxon signed-rank test. Area under the receiver operating characteristic curve (AROC) with 95% confidence interval was used to assess the diagnostic ability of structural FAZ metrics, functional FAZ metrics, FAZ perimeter and acircularity index change (functional FAZ – structural FAZ), and FAZ area enlargements to differentiate between eyes without diabetic retinopathy (control + noDR) and with diabetic retinopathy (NPDR + PDR).

3. Results

3.1 Subjects

A total of 117 subjects were recruited in this study. After excluding 8 diabetic patients due to the presence of exudates and/or significant macular edema at the FAZ border, 109 subjects (20 healthy controls, 26 noDR, 25 NPDR, and 38 PDR) were included for data analysis. There were no significant differences in age (P = 0.09) or axial length (P = 0.09) among the 4 study groups. Subject demographic data are displayed in Table 1.

Table 1. Demographic data of the 4 study groups.

Group	No. of Subjects	Male/Female	Age (Mean ± SD, years)	Diabetes Type 1/Type 2
Control	20	8/12	50.9 ± 10.5	NA
noDR	26	21/5	56.8 ± 9.5	1/25
NPDR	25	11/14	54.8 ± 8.6	5/20
PDR	38	19/19	52.3 ± 10.0	7/31

3.2 FAZ delineation - intergrader repeatability

On the structural FAZ, measurements of FAZ area, perimeter, and acircularity index were highly correlated between the two graders, with an ICC of 0.999 (95% confidence interval, 0.998-0.999), 0.986 (95% confidence interval, 0.980-0.991), and 0.949 (95% confidence interval, 0.926-0.965), respectively. On the functional FAZ, measurement of FAZ area ICC was of 1.000 (95% confidence interval, 1.000-1.000), perimeter was 0.999 (95% confidence interval, 0.998-0.999), and acircularity index was 0.995 (95% confidence interval, 0.993-0.997). Between the two graders, Bland-Altman plots showed that the mean ± SD differences for structural FAZ area, perimeter, and acircularity index were –0.003 ± 0.007mm^2, –0.024 ± 0.100mm, –0.006 ± 0.048, respectively, whereas the mean ± SD differences for functional FAZ area, perimeter, and acircularity index were 0.003 ± 0.003mm^2, 0.013 ± 0.077mm, and –0.003 ± 0.035, respectively.

3.3 Structural and functional FAZ metrics

Boxplots of the structural and functional FAZ metrics are shown in Fig. 3. There was no statistically significant difference between groups in structural FAZ area (P = 0.07; Fig. 3(A)) and structural FAZ acircularity index (P = 0.3; Fig. 3(C)). However, structural FAZ perimeter was significantly greater in the PDR group when compared to the control group (Fig. 3(B)). In contrast, significant differences among groups were observed in all functional FAZ metrics. Functional FAZ area was significantly greater in the PDR group when compared to the control and noDR groups (Fig. 3(D)). Functional FAZ perimeter was significantly greater in the PDR group in comparison to the control, noDR, and NPDR groups (Fig. 3(E)). Also, the functional FAZ area was larger in the NPDR group in comparison to the control group. Similarly, functional FAZ aicircularity index was significantly greater in the PDR group compared to control and noDR groups. Functional FAZ acircularity index was also significantly larger in the NPDR group in comparison to the NoDR group (Fig. 3(F)).

Biomedical Optics EXPRESS

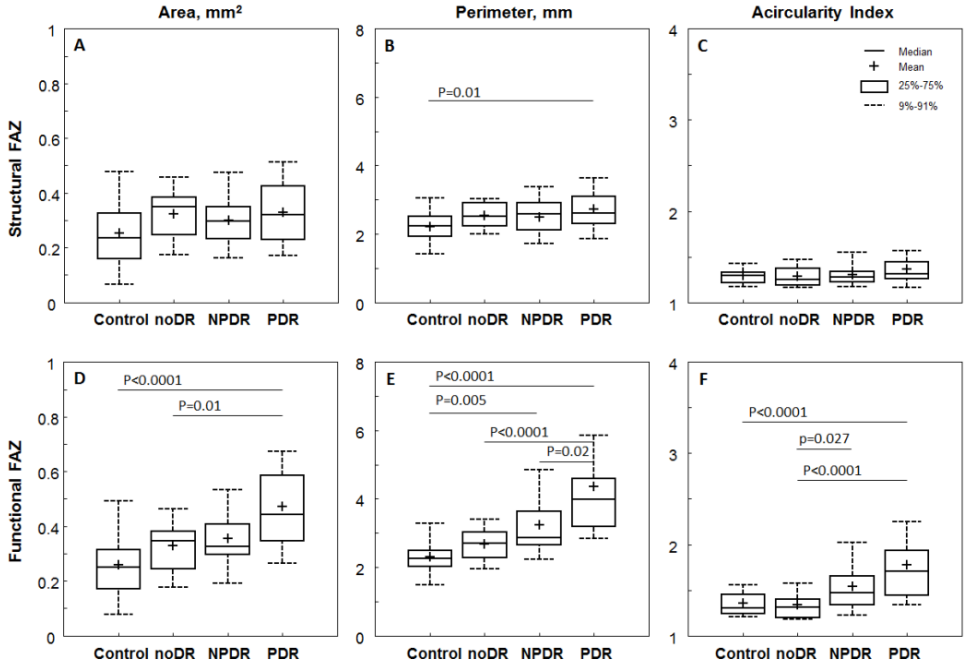

Fig. 3. Boxplots of the structural (top row) and functional (bottom row) FAZ metrics across 4 study groups. (A & D) FAZ area. (B & E) FAZ perimeter. (C & F) FAZ acircularity index. Significant P-values for the post-hoc pairwise comparisons after nonparametric Kruskal-Wallis tests are shown; all other comparisons were not significant (P>0.05).

3.4 Within-subject FAZ area enlargements

There was no statistical significant difference between the structural and functional FAZ area in the control group (P = 0.079). Boxplots of the total and quadrant FAZ area enlargement are shown in Fig. 4. Our findings showed that FAZ area enlargements increased with worsening diabetic retinopathy. In particular, total FAZ area enlargement was significantly higher in the PDR and NPDR groups compared to the control and noDR groups (Fig. 4(A)). The largest total FAZ area enlargement was found in the PDR group with mean ± SD of 0.15 ± 0.17mm^2, followed by the NPDR (0.06 ± 0.06mm^2), noDR (0.01 ± 0.01mm^2), and control (0.01 ± 0.01mm^2). No significant differences between the control and noDR groups were observed. Similar relationships were observed in the four quadrants (Fig. 4(B)-(E)) and four hemifields (boxplots not shown).

In quadrant analysis, the largest FAZ area enlargement was found in the nasal quadrant (0.020 ± 0.057mm^2), followed by the superior (0.020 ± 0.041mm^2), inferior (0.017 ± 0.032mm^2), and temporal (0.015 ± 0.025mm^2) quadrants. The same trend was also found in hemifield analysis with the largest FAZ area enlargement observed in the nasal hemifield (0.038 ± 0.086mm^2), followed by the superior (0.038 ± 0.069mm^2), inferior (0.034 ± 0.060mm^2), and temporal (0.033 ± 0.047mm^2) hemifields. However, none of the differences between the opposite quadrants and hemifields were significant (Wilcoxon signed-rank tests: temporal vs nasal quadrant, P = 0.74; superior vs inferior quadrant, P = 0.31; temporal vs nasal hemifield, P = 0.93; superior vs inferior hemifield, P = 0.38). Hemifield FAZ area enlargement difference in each subject is shown in Fig. 5.

Biomedical Optics EXPRESS

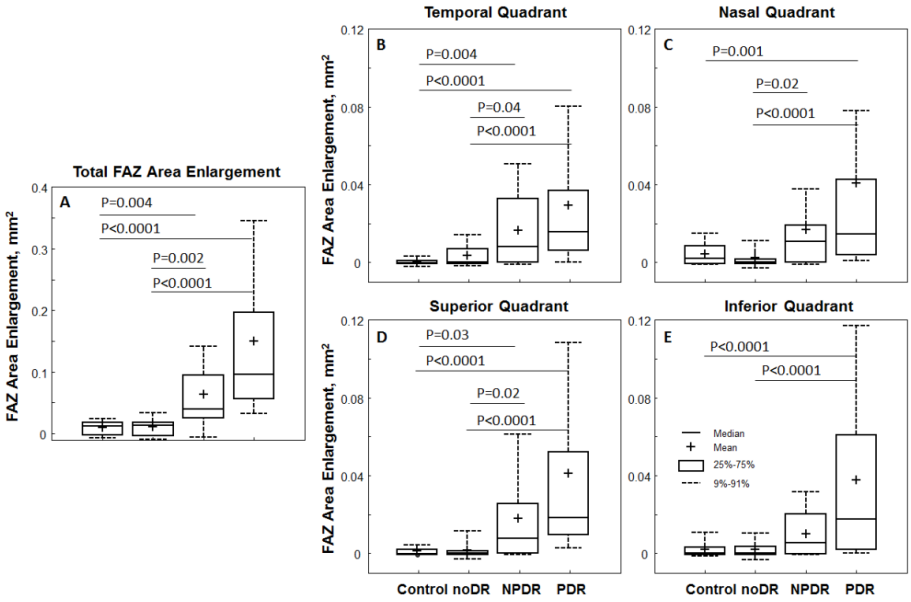

Fig. 4. Boxplots of within-subject FAZ area enlargement across 4 study groups. (A) Total FAZ area enlargement. (B) Temporal quadrant. (C) Nasal quadrant. (D) Superior quadrant. (E) Inferior quadrant. Significant P-values for the post-hoc pairwise comparisons after nonparametric Kruskal-Wallis tests are shown; all other comparisons were not significant (P>0.05).

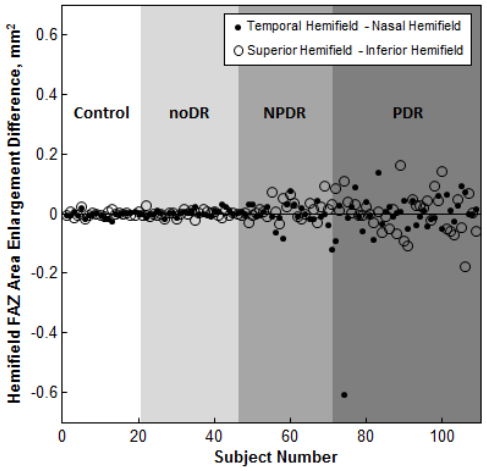

Fig. 5. FAZ area enlargement difference for hemifields in each subject (filled circles: temporal-nasal hemifield and open circles: superior-inferior hemifield). Our findings suggested that FAZ area enlargement is neither quadrant nor hemifield specific in diabetic retinopathy.

3.5 Area under the receiver operating characteristic curve (AROC)

The results of the AROC analyses for structural FAZ metrics, functional FAZ metrics, FAZ perimeter and acircularity index change, and FAZ area enlargements are shown in Table 2. Unlike structural FAZ metrics, which showed nearly no diagnostic capability, functional FAZ metrics demonstrated good diagnostic capability of 0.73-0.84 AROC when differentiating between eyes with and without diabetic retinopathy. The total FAZ area enlargement showed the highest AROC of 0.91 with 81% sensitivity at 95% specificity and 32.6% specificity at 95% sensitivity, indicating an excellent diagnostic accuracy (Fig. 6).

Biomedical Optics EXPRESS

Table 2. Area under the receiver operating characteristic (AROC) curve analyses of the structural FAZ, functional FAZ, FAZ perimeter and acircularity index change, and FAZ area enlargement in differentiating eyes with diabetic retinopathy (NPDR + PDR) and eyes without diabetic retinopathy (Control + noDR).

	Measurements		AROC (95% Confidence Interval)
Structural FAZ	Area		0.55 (0.44-0.66)
	Perimeter		0.61 (0.50-0.71)
	Acircularity Index		0.58 (0.47-0.69)
Functional FAZ	Area		0.73 (0.64-0.83)
	Perimeter		0.84 (0.77-0.91)
	Acircularity Index		0.81 (0.73-0.89)
FAZ Perimeter Change			0.85 (0.78-0.92)
FAZ Acircularity Index Change			0.79 (0.70-0.87)
FAZ Area Enlargement	Total Enlargement		0.91 (0.85-0.97)
	Quadrant	Temporal	0.82 (0.74-0.90)
		Nasal	0.79 (0.70-0.87)
		Superior	0.85 (0.78-0.92)
		Inferior	0.78 (0.69-0.86)
	Hemifield	Temporal	0.88 (0.81-0.94)
		Nasal	0.84 (0.76-0.91)
		Superior	0.88 (0.81-0.94)
		Inferior	0.81 (0.73-0.89)

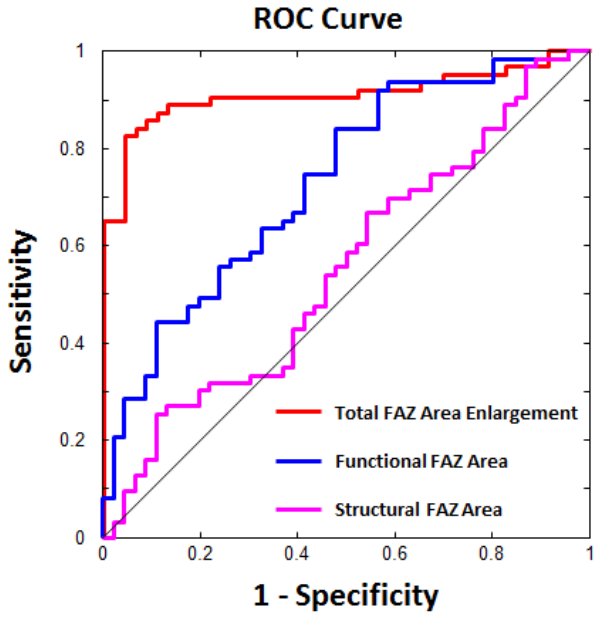

Fig. 6. Diagnostic ability of structural FAZ area, functional FAZ area, and total FAZ area enlargement for discriminating eyes with and without diabetic retinopathy. Total FAZ area enlargement showed the largest AROC of 0.91 (red), followed by functional FAZ area of 0.73 (blue) and structural FAZ area of 0.55 (magenta).

3.6 Identification of nonperfused capillaries

Nonperfused capillaries were identified in all 4 study groups. Figure 7 demonstrates nonperfused capillary segments visualized as hypo-reflective cord-like structures around the FAZ on the contrast-inverted *en face* OCT reflectance images (top row, red arrows).

Biomedical Optics EXPRESS

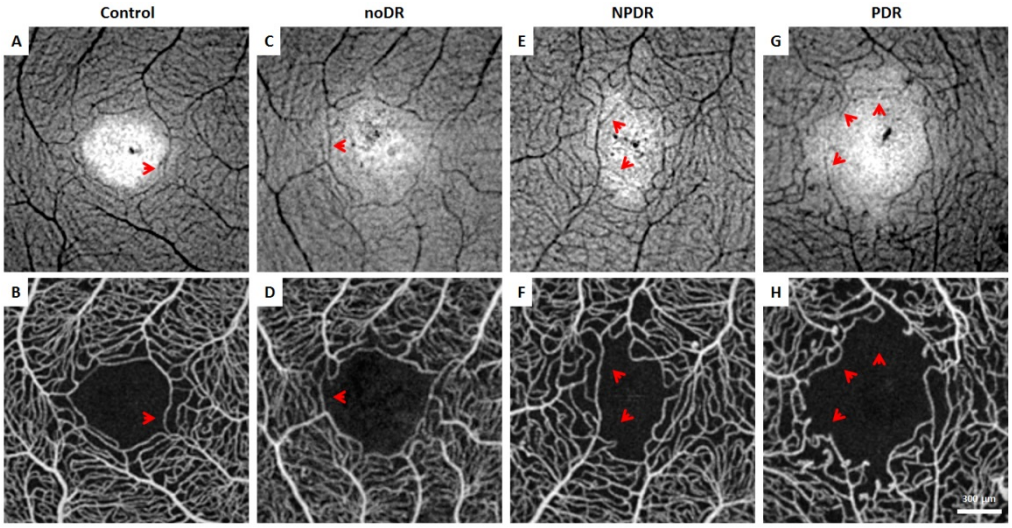

Fig. 7. Contrast-inverted *en face* OCT reflectance (top row) and OCT angiograph (bottom row) in a (A & B) healthy control, (C & D) noDR subject, (E & F) NPDR subject, and (G & H) PDR subject. Red arrows indicate non-perfused capillary segments identified as hypo-reflective cord-like structure on the contrast-inverted OCT reflectance that was absent on the corresponding OCT angiography images.

4. Discussion

In this study, we have demonstrated the feasibility of measuring FAZ area enlargement within an individual eye by comparing the structural and functional FAZs delineated on the simultaneously-acquired, corresponding averaged *en face* OCT reflectance and OCT angiography images.

4.1 Structural and functional FAZ metrics

In agreement with prior IVFA and OCT angiography studies, we found that functional FAZ metrics increased with worsening diabetic retinopathy [9,12,25,42]. In particular, the PDR group showed significantly larger functional FAZ area, perimeter, and acircularity index compared to the control and noDR groups (Fig. 3, bottom row). Notably, our finding of functional FAZ area also showed considerable variability in healthy controls [43–46] with substantial overlap between the control and diabetic groups [13]. In contrast, there was no significant difference in structural FAZ area and acircularity index among the 4 study groups (Fig. 3(A) & 3(C)). This demonstrates how the *en face* scan can be used to reveal the original anatomical FAZ before the onset of capillary nonperfusion or intraluminal remodeling due to diabetic retinopathy. Interestingly, structural FAZ perimeter was found to be significantly larger in the PDR group compared to the control group, possibly due to the increased capillary tortuosity at the FAZ border before capillary nonperfusion occurs in advanced cases of diabetic retinopathy with capillary remodeling or neovascularization (Fig. 3(B)).

4.2 Within-subject FAZ area enlargements

Enlargement of FAZ due to capillary nonperfusion is associated with significant visual loss in patients with diabetic retinopathy [14–16], and has shown to be a prognostic indicator of disease severity [7,24,47]. Previous histopathological studies of diabetic retina have reported that the frequency of diabetic vascular lesions was significantly higher in the temporal retina than in the nasal retina [48,49]. Similarly, prior clinical studies using wide-field color fundus photography have suggested a non-uniform distribution of diabetic lesions favoring the temporal retina compared to the nasal retina [50]. It might be therefore expected that the

Biomedical Optics EXPRESS

temporal side of the FAZ would be more vulnerable to capillary nonperfusion due to diabetic retinopathy, resulting in a preferential expansion of the FAZ area in the temporal quadrant or temporal hemifield. Our findings, however, reveal no quadrant or hemifield bias of FAZ area enlargement. There were no statistical significant differences between the opposite quadrants or hemifields (Figs. 4 and 5), implying that capillary nonperfusion at the FAZ border occurs randomly in any of the four quadrants or hemifields as diabetic retinopathy advances. The discrepancy is possibly due to the difference in retinal thickness in the regions studied, with the midperiphery used in prior studies versus the parafoveal region in the current study. Maximum macular thickness is found within the 3 mm diameter of the parafovea, while the thinnest retina is observed in the temporal retina decreasing gradually toward the periphery [51]. This relative thinness of temporal retina beyond the center 3 mm of the macula may contribute to greater vulnerability to ischemia and hence diabetic changes [52]. Wide-field fluorescein angiography appears to also support this increased susceptibility of the temporal midperipheral retina to diabetic changes. The uniform FAZ area enlargement found in the current study was measured at the parafoveal region using 3x3 mm OCT reflectance and OCT angiography images. This 3x3 mm parafoveal region has relatively uniform and symmetrical retinal thickness, resulting in a different perspective than the non-uniform distribution of diabetic changes of the asymmetric midperiphery. Parafoveal OCT angiography used in a recent study similarly reported that capillary nonperfusion occurs in any area of the macula without any quadrant bias in diabetic retinopathy [53].

4.3 Area under the receiver operating characteristic curve (AROC)

For distinguishing between eyes with retinopathy (NPDR and PDR groups) and eyes without retinopathy (control and NoDR groups), total FAZ area enlargement measured within the same individual showed the greatest diagnostic capability compared to the structural FAZ metrics and functional FAZ metrics (Table 2 & Fig. 6). Since the measurement of FAZ area enlargement was computed using the structural FAZ as a baseline before the onset of capillary nonperfusion, it is understandable that the substantial individual variation found in FAZ area alone is eliminated, leading to a more sensitive and effective diagnostic capability compared to other FAZ metrics.

4.4 Identification of nonperfused capillaries

Identification of perfused and nonperfused capillaries is key in understanding microvascular changes from the onset of diabetic retinopathy to progression. In this study, we have demonstrated that co-registration of the simultaneously-acquired, corresponding *en face* OCT reflectance and OCT angiography images provides both structural and functional information of perfused and nonperfused capillaries. One of the necessary conditions for recanalization of nonperfused capillaries is the presence of intact capillary structure. Identification of nonperfused capillary structure on the OCT reflectance may therefore indicate the potential to recanalize, which could help predict and monitor possible structural benefits of treatment intervention along with the perfusion status on the OCT angiography images [29]. While capillary nonperfusion was characteristically visualized in all PDR patients, it is important to note that the occurrence of nonperfused capillary segments in healthy individuals is not uncommon (Fig. 7(A) & 7(B)). Using adaptive optics and OCT angiography, prior studies have shown that at least one nonperfused capillary segment was identified in 31%-42% of healthy controls, as normal variants or due to aging [29,54].

4.5 Limitations

There are a number of limitations to this study. Patients were excluded if the structural or functional FAZ border was distorted or obscured by the presence of exudate or severe macular edema, thus restricting the clinical implications of the study to eyes with minimal diabetic macular disease (Fig. 8). In patients with PDR who developed parafoveal

Biomedical Optics EXPRESS

neovascularization at the FAZ border, the structural FAZ might misrepresent the baseline anatomical FAZ (Fig. 8). Additionally, capillaries identified as being nonperfused may actually contain slow blood flow rather than complete occlusion due to the velocity detection threshold of the software; this may result in an overestimation of FAZ area enlargement [55]. While intergrader agreement for both structural and functional FAZ segmentations was excellent, manual segmentation is a laborious process and is not clinically practical. Finally, the process of acquiring 10 consecutive scans is time-consuming and limited by patient cooperation and operator skill.

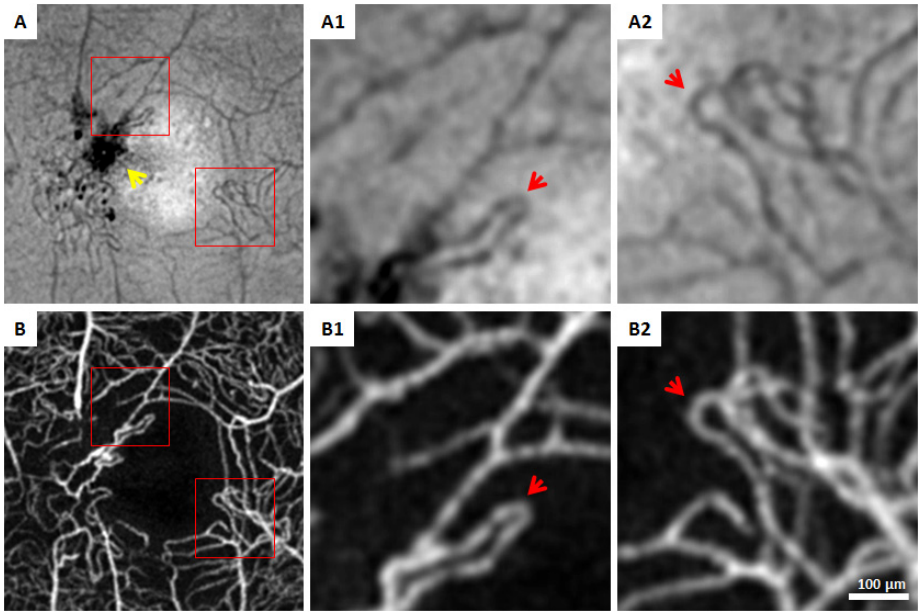

Fig. 8. The presence of exudates and neovascularization at the FAZ border in the right eye of a PDR patient. (A & B) Structural FAZ border was obscured by the presence of exudates on the contrast-inverted *en face* OCT reflectance (yellow arrow), while a complete functional FAZ border was visualized on the OCT angiography image. Magnified images of the red boxes are shown in A1-2 and B1-2. Red arrows indicate neovascularization across the true structural FAZ border, which falsely represent the anatomical FAZ border before the onset of diabetic retinopathy. This patient was excluded from image analysis.

5. Conclusions

Comparison of simultaneously-acquired, corresponding *en face* OCT reflectance to OCT angiography images is a useful technique for studying the structural versus functional FAZ. The baseline anatomic architecture revealed by *en face* OCT reflectance is a helpful guide for more accurate assessment disease severity and progression within an individual eye. Total FAZ area enlargement appears to be a more sensitive marker for identifying eyes with diabetic retinopathy compared to measuring FAZ area on OCT angiography images alone, which may prove useful for recognizing the earlier onset of diabetic retinal change.

Funding

National Eye Institute of the National Institutes of Health (R01EY027301, R01EY024969 and P30EY001931). The content is solely the responsibility of the authors and does not necessarily represent the official views of the National Institutes of Health. Additional funding for this research was provided by the New York Eye and Ear Infirmary Foundation Grant, Marrus Family Foundation, the Geraldine Violett Foundation, The Edward N. & Della L. Thome Memorial Foundation, and the Jorge N. Buxton Microsurgical Foundation. The sponsors and funding organizations had no role in the design or conduct of this research.

Biomedical Optics EXPRESS

Acknowledgments

The authors thank Erin Curran for her assistance with the study.

Disclosures

RBR: Optovue (C); Boehringer-Ingelheim (C); Astellas (C); Genentech-Roche (C); NanoRetina (C); OD-OS (C); Opticology (I); Guardion (I); GlaucoHealth: (I); Regeneron (C); Bayer (C). JC: Optovue (F).

References

1. N. Cheung, P. Mitchell, and T. Y. Wong, "Diabetic retinopathy," Lancet **376**(9735), 124–136 (2010).
2. M. E. Hartnett, W. Baehr, and Y. Z. Le, "Diabetic retinopathy, an overview," Vision Res. **139**, 1–6 (2017).
3. E. J. Duh, J. K. Sun, and A. W. Stitt, "Diabetic retinopathy: Current understanding, mechanisms, and treatment strategies," JCI Insight **2**(14), e93751 (2017).
4. S. Sivaprasad, B. Gupta, R. Crosby-Nwaobi, and J. Evans, "Prevalence of diabetic retinopathy in various ethnic groups: A worldwide perspective," Surv. Ophthalmol. **57**(4), 347–370 (2012).
5. N. Takase, M. Nozaki, A. Kato, H. Ozeki, M. Yoshida, and Y. Ogura, "Enlargement of foveal avascular zone in diabetic eyes evaluated by en face optical coherence tomography angiography," Retina **35**(11), 2377–2383 (2015).
6. Y. Lu, J. M. Simonett, J. Wang, M. Zhang, T. Hwang, A. M. Hagag, D. Huang, D. Li, and Y. Jia, "Evaluation of automatically quantified foveal avascular zone metrics for diagnosis of diabetic retinopathy using optical coherence tomography angiography," Invest. Ophthalmol. Vis. Sci. **59**(6), 2212–2221 (2018).
7. R. Mastropasqua, L. Toto, A. Mastropasqua, R. Aloia, C. De Nicola, P. A. Mattei, G. Di Marzio, M. Di Nicola, and L. Di Antonio, "Foveal avascular zone area and parafoveal vessel density measurements in different stages of diabetic retinopathy by optical coherence tomography angiography," Int. J. Ophthalmol. **10**(10), 1545–1551 (2017).
8. P. L. Nesper, P. K. Roberts, A. C. Onishi, H. Chai, L. Liu, L. M. Jampol, and A. A. Fawzi, "Quantifying microvascular abnormalities with increasing severity of diabetic retinopathy using optical coherence tomography angiography," Invest. Ophthalmol. Vis. Sci. **58**(6), BIO307 (2017).
9. D. Bhanushali, N. Anegondi, S. G. Gadde, P. Srinivasan, L. Chidambara, N. K. Yadav, and A. Sinha Roy, "Linking retinal microvasculature features with severity of diabetic retinopathy using optical coherence tomography angiography," Invest. Ophthalmol. Vis. Sci. **57**(9), OCT519 (2016).
10. S. A. Agemy, N. K. Scripsema, C. M. Shah, T. Chui, P. M. Garcia, J. G. Lee, R. C. Gentile, Y. S. Hsiao, Q. Zhou, T. Ko, and R. B. Rosen, "Retinal vascular perfusion density mapping using optical coherence tomography angiography in normals and diabetic retinopathy patients," Retina **35**(11), 2353–2363 (2015).
11. Early Treatment Diabetic Retinopathy Study Research Group, "Classification of diabetic retinopathy from fluorescein angiograms. ETDRS report number 11," Ophthalmology **98**(5l), 807–822 (1991).
12. G. H. Bresnick, R. Condit, S. Syrjala, M. Palta, A. Groo, and K. Korth, "Abnormalities of the foveal avascular zone in diabetic retinopathy," Arch. Ophthalmol. **102**(9), 1286–1293 (1984).
13. J. Conrath, R. Giorgi, D. Raccah, and B. Ridings, "Foveal avascular zone in diabetic retinopathy: Quantitative vs qualitative assessment," Eye (Lond.) **19**(3), 322–326 (2005).
14. C. Balaratnasingam, M. Inoue, S. Ahn, J. McCann, E. Dhrami-Gavazi, L. A. Yannuzzi, and K. B. Freund, "Visual acuity is correlated with the area of the foveal avascular zone in diabetic retinopathy and retinal vein occlusion," Ophthalmology **123**(11), 2352–2367 (2016).
15. F. Tang, Z. Sun, R. Wong, J. Lok, A. Lam, C. C. Tham, C. K. Chan, S. Mohamed, T. C. Lam, S. K. Szeto, D. S. Ng, and C. Y. Cheung, "Relationship of intercapillary area with visual acuity in diabetes mellitus: An optical coherence tomography angiography study," Br. J. Ophthalmol. 312010 (2018).
16. K. Sakata, H. Funatsu, S. Harino, H. Noma, and S. Hori, "Relationship of macular microcirculation and retinal thickness with visual acuity in diabetic macular edema," Ophthalmology **114**(11), 2061–2069 (2007).
17. The Diabetes Control and Complications Trial Research Group, "Color photography vs fluorescein angiography in the detection of diabetic retinopathy in the diabetes control and complications trial," Arch. Ophthalmol. **105**(10), 1344–1351 (1987).
18. T. J. Ffytche, J. S. Shilling, I. H. Chisholm, and J. L. Federman, "Indications for fluorescein angiography in disease of the ocular fundus: A review," J. R. Soc. Med. **73**(5), 362–365 (1980).
19. K. R. Mendis, C. Balaratnasingam, P. Yu, C. J. Barry, I. L. McAllister, S. J. Cringle, and D. Y. Yu, "Correlation of histologic and clinical images to determine the diagnostic value of fluorescein angiography for studying retinal capillary detail," Invest. Ophthalmol. Vis. Sci. **51**(11), 5864–5869 (2010).
20. R. F. Spaide, J. M. Klancnik, Jr., and M. J. Cooney, "Retinal vascular layers imaged by fluorescein angiography and optical coherence tomography angiography," JAMA Ophthalmol. **133**(1), 45–50 (2015).
21. D. A. Salz and A. J. Witkin, "Imaging in diabetic retinopathy," Middle East Afr. J. Ophthalmol. **22**(2), 145–150 (2015).

Biomedical Optics EXPRESS

22. D. A. Dmuchowska, P. Krasnicki, and Z. Mariak, "Can optical coherence tomography replace fluorescein angiography in detection of ischemic diabetic maculopathy?" Graefes Arch. Clin. Exp. Ophthalmol. **252**(5), 731–738 (2014).
23. G. Cennamo, M. R. Romano, G. Nicoletti, N. Velotti, and G. de Crecchio, "Optical coherence tomography angiography versus fluorescein angiography in the diagnosis of ischaemic diabetic maculopathy," Acta Ophthalmol. **95**(1), e36–e42 (2017).
24. F. J. Freiberg, M. Pfau, J. Wons, M. A. Wirth, M. D. Becker, and S. Michels, "Optical coherence tomography angiography of the foveal avascular zone in diabetic retinopathy," Graefes Arch. Clin. Exp. Ophthalmol. **254**(6), 1051–1058 (2016).
25. T. S. Hwang, A. M. Hagag, J. Wang, M. Zhang, A. Smith, D. J. Wilson, D. Huang, and Y. Jia, "Automated quantification of nonperfusion areas in 3 vascular plexuses with optical coherence tomography angiography in eyes of patients with diabetes," JAMA Ophthalmol. **136**(8), 929–936 (2018).
26. G. Di, Y. Weihong, Z. Xiao, Y. Zhikun, Z. Xuan, Q. Yi, and D. Fangtian, "A morphological study of the foveal avascular zone in patients with diabetes mellitus using optical coherence tomography angiography," Graefes Arch. Clin. Exp. Ophthalmol. **254**(5), 873–879 (2016).
27. D. Y. Kim, J. Fingler, R. J. Zawadzki, S. S. Park, L. S. Morse, D. M. Schwartz, S. E. Fraser, and J. S. Werner, "Noninvasive imaging of the foveal avascular zone with high-speed, phase-variance optical coherence tomography," Invest. Ophthalmol. Vis. Sci. **53**(1), 85–92 (2012).
28. A. Ishibazawa, T. Nagaoka, A. Takahashi, T. Omae, T. Tani, K. Sogawa, H. Yokota, and A. Yoshida, "Optical coherence tomography angiography in diabetic retinopathy: A prospective pilot study," Am. J. Ophthalmol. **160**(1), 35–44 (2015).
29. B. D. Krawitz, E. Phillips, R. D. Bavier, S. Mo, J. Carroll, R. B. Rosen, and T. Y. P. Chui, "Parafoveal nonperfusion analysis in diabetic retinopathy using optical coherence tomography angiography," Transl. Vis. Sci. Technol. **7**(4), 4 (2018).
30. A. Uji, S. Balasubramanian, J. Lei, E. Baghdasaryan, M. Al-Sheikh, and S. R. Sadda, "Impact of multiple en face image averaging on quantitative assessment from optical coherence tomography angiography images," Ophthalmology **124**(7), 944–952 (2017).
31. T. G. Schmidt, R. Linderman, M. Strampe, T. Y. P. Chui, R. B. Rosen, and J. Carroll, "The utility of frame averaging for automated algorithms in analyzing retinal vascular biomarkers in AngioVue OCTA," Transl. Vis. Sci. Technol. (in review).
32. R. B. Rosen, M. Hathaway, J. Rogers, J. Pedro, P. Garcia, P. Laissue, G. M. Dobre, and A. G. Podoleanu, "Multidimensional en-face OCT imaging of the retina," Opt. Express **17**(5), 4112–4133 (2009).
33. Y. Miwa, T. Murakami, K. Suzuma, A. Uji, S. Yoshitake, M. Fujimoto, T. Yoshitake, Y. Tamura, and N. Yoshimura, "Relationship between functional and structural changes in diabetic vessels in optical coherence tomography angiography," Sci. Rep. **6**(1), 29064 (2016).
34. A. Uji, S. Balasubramanian, J. Lei, E. Baghdasaryan, M. Al-Sheikh, and S. R. Sadda, "Choriocapillaris imaging using multiple en face optical coherence tomography angiography image averaging," JAMA Ophthalmol. **135**(11), 1197–1204 (2017).
35. Early Treatment Diabetic Retinopathy Study Research Group, "Grading diabetic retinopathy from stereoscopic color fundus photographs–an extension of the modified airlie house classification. ETDRS report number 10. Early treatment diabetic retinopathy study research group," Ophthalmology **98**, 786–806 (1991).
36. Early Treatment Diabetic Retinopathy Study Research Group, "Fundus photographic risk factors for progression of diabetic retinopathy. ETDRS report number 12," Ophthalmology **98**(5), 823–833 (1991).
37. A. G. Bennett, A. R. Rudnicka, and D. F. Edgar, "Improvements on Littmann's method of determining the size of retinal features by fundus photography," Graefes Arch. Clin. Exp. Ophthalmol. **232**(6), 361–367 (1994).
38. S. Mo, E. Phillips, B. D. Krawitz, R. Garg, S. Salim, L. S. Geyman, E. Efstathiadis, J. Carroll, R. B. Rosen, and T. Y. Chui, "Visualization of radial peripapillary capillaries using optical coherence tomography angiography: The effect of image averaging," PLoS One **12**(1), e0169385 (2017).
39. Y. Jia, O. Tan, J. Tokayer, B. Potsaid, Y. Wang, J. J. Liu, M. F. Kraus, H. Subhash, J. G. Fujimoto, J. Hornegger, and D. Huang, "Split-spectrum amplitude-decorrelation angiography with optical coherence tomography," Opt. Express **20**(4), 4710–4725 (2012).
40. C. A. Schneider, W. S. Rasband, and K. W. Eliceiri, "NIH Image to ImageJ: 25 years of image analysis," Nat. Methods **9**(7), 671–675 (2012).
41. I. Arganda-Carreras, C. O. S. Sorzano, R. Marabini, J. M. Carazo, C. Ortiz-de-Solorzano, and J. Kybic, "Consistent and elastic registration of histological sections using vector-spline regularization," in *Computer Vision Approaches to Medical Image Analysis* (Springer Berlin Heidelberg, 2006), 85–95.
42. B. D. Krawitz, S. Mo, L. S. Geyman, S. A. Agemy, N. K. Scripsema, P. M. Garcia, T. Y. P. Chui, and R. B. Rosen, "Acircularity index and axis ratio of the foveal avascular zone in diabetic eyes and healthy controls measured by optical coherence tomography angiography," Vision Res. **139**, 177–186 (2017).
43. T. Y. Chui, D. A. VanNasdale, A. E. Elsner, and S. A. Burns, "The association between the foveal avascular zone and retinal thickness," Invest. Ophthalmol. Vis. Sci. **55**(10), 6870–6877 (2014).
44. L. Z. Wu, Z. S. Huang, D. Z. Wu, and E. Chan, "Characteristics of the capillary-free zone in the normal human macula," Jpn. J. Ophthalmol. **29**(4), 406–411 (1985).

Biomedical Optics EXPRESS

45. G. N. Magrath, E. A. T. Say, K. Sioufi, S. Ferenczy, W. A. Samara, and C. L. Shields, "Variability in foveal avascular zone and capillary density using optical coherence tomography angiography machines in healthy eyes," Retina **37**(11), 2102–2111 (2017).
46. L. Laatikainen and J. Larinkari, "Capillary-free area of the fovea with advancing age," Invest. Ophthalmol. Vis. Sci. **16**(12), 1154–1157 (1977).
47. K. Ghasemi Falavarjani, N. A. Iafe, J. P. Hubschman, I. Tsui, S. R. Sadda, and D. Sarraf, "Optical coherence tomography angiography analysis of the foveal avascular zone and macular vessel density after anti-vegf therapy in eyes with diabetic macular edema and retinal vein occlusion," Invest. Ophthalmol. Vis. Sci. **58**(1), 30–34 (2017).
48. J. Tang, S. Mohr, Y. D. Du, and T. S. Kern, "Non-uniform distribution of lesions and biochemical abnormalities within the retina of diabetic humans," Curr. Eye Res. **27**(1), 7–13 (2003).
49. T. S. Kern and R. L. Engerman, "Vascular lesions in diabetes are distributed non-uniformly within the retina," Exp. Eye Res. **60**(5), 545–549 (1995).
50. P. S. Silva, J. D. Cavallerano, J. K. Sun, A. Z. Soliman, L. M. Aiello, and L. P. Aiello, "Peripheral lesions identified by mydriatic ultrawide field imaging: Distribution and potential impact on diabetic retinopathy severity," Ophthalmology **120**(12), 2587–2595 (2013).
51. A. Chan, J. S. Duker, T. H. Ko, J. G. Fujimoto, and J. S. Schuman, "Normal macular thickness measurements in healthy eyes using Stratus optical coherence tomography," Arch. Ophthalmol. **124**(2), 193–198 (2006).
52. J. Jiang, Y. Liu, Y. Chen, B. Ma, Y. Qian, Z. Zhang, D. Zhu, Z. Wang, and X. Xu, "Analysis of changes in retinal thickness in type 2 diabetes without diabetic retinopathy," J. Diabetes Res. **2018**, 3082893 (2018).
53. Y. Kaizu, S. Nakao, S. Yoshida, T. Hayami, M. Arima, M. Yamaguchi, I. Wada, T. Hisatomi, Y. Ikeda, T. Ishibashi, and K. H. Sonoda, "Optical coherence tomography angiography reveals spatial bias of macular capillary dropout in diabetic retinopathy," Invest. Ophthalmol. Vis. Sci. **58**(11), 4889–4897 (2017).
54. A. Pinhas, M. Razeen, M. Dubow, A. Gan, T. Y. Chui, N. Shah, M. Mehta, R. C. Gentile, R. Weitz, J. B. Walsh, Y. N. Sulai, J. Carroll, A. Dubra, and R. B. Rosen, "Assessment of perfused foveal microvascular density and identification of nonperfused capillaries in healthy and vasculopathic eyes," Invest. Ophthalmol. Vis. Sci. **55**(12), 8056–8066 (2014).
55. R. F. Spaide, J. G. Fujimoto, and N. K. Waheed, "Image artifacts in optical coherence tomography angiography," Retina **35**(11), 2163–2180 (2015).